Anonymous Referee #1
Received and published: 11 October 2018

> General comments:
> This paper presents a DNS study on droplet growth by condensation in turbulence. The purpose of this study is to explore the influence of supersaturation fluctuation on the broadening of droplet size distribution and to investigate the Reynolds number dependency of the broadening. The microphysics is solved by using the Lagrangian superdroplet method. By comparing the numerical results from the condensation at different Reynolds numbers and dissipation rates, the authors concluded that the supersaturation fluctuations produce broader droplet size distributions. The manuscript represents a good contribution to the development of new theories for the condensation process and is of potential interest for Atmospheric Chemistry and Physics community. However, by careful reading, some arguments in the context may seem hand-waving and are not sufficiently robust to derive the main conclusion, and the evidence that the authors have cited are not firmly supportive. I would suggest that the authors provide more physical explanations and plots for the arguments. I would support the publication of this paper after the authors consider carefully the comments listed below.

We thank the reviewer for his/her constructive remarks. As explained below in detail, we have now tried to make our arguments more robust. All our changes are highlighted in blue.

Specific comments:
> -Page 6/line 16: My main and critical points to the employed numerical framework is the choice of the timestep. It is not true that the Kolmogorov time scale is the smallest of the system. For 10 micrometres droplet, the particle response time defined in equation (15) is several order of magnitude lower. Unphysical droplet trajectories can be generated used such a large time step. Which temporal integration scheme is employed to solve equation (14)? Saito Gotoh used an implicit scheme and nevertheless their time step is much smaller than the Kolmogorov time scale. Can the authors comment on this issue? A validation case must be provided (at least for one of the low-resolution cases) with a much smaller time step. If the results differ, an entirely new dataset must be generated for the paper.

The smallest physical time step in the system is indeed the particle response time. This was always handled correctly in the code, but we didn't describe this correctly. We have now corrected the text in the first paragraph of section 3.1 on page 7. A validation is provided in the response as supplementary material.
Since our simulation time step is smaller than the smallest physical time step, a shorter time step gives identical results.

> -If the time step is the Kolmogorov time scale, why is the maximum time of simulation limited to 80 s? The maximum number of iterations will be 4000 that is not so difficult to reach in a supercomputer with few hours of computational time.

As explained above, the smallest time step in the system is indeed the particle response time. We have now corrected the text in the first paragraph of section 3.1 on page 7. A validation is provided in the response.

> -Why do you evolve superparticles? Can the authors not evolve the actual number of particles inside the domain? The maximum number of droplets that need to be evolved is about 30 million that again is not so prohibitive in a modern supercomputer. State of the art of droplet-laden DNS has reached much higher droplet numbers. -Connecting the previous points: How long computational time is needed for the smaller and the larger case? How many cores have you used?

We emphasized in lines 22-26 on page 3 that "For condensational growth, the superparticle approach (Li et al., 2017) is the same as the Lagrangian point-particle approach (Kumar et al., 2014) since there is no

interactions among droplets. Nevertheless, we still use the superparticle
approach so that we can include more processes like collection (Li et al.,
2017, 2018) in future. Another reason to adopt superparticle approach
is that it can be easily adapted to conduct Large-eddy simulations with
appropriate sub-grid scale models (Grabowski and Abade, 2017)."

We have now added the description of the CPU cost at the end
of section 3.2 on page 7.

> -Page 1/l. 7-8: the adverbs "strongly" and "weakly" (which also
> appear in other parts of the manuscript) are not fully supported by the
> results provided in the paper. I can see differences below one order
> of magnitude smaller between the lines in the plots (e.g. Fig. 4). The
> range of Reynolds number is quite limited to appreciate "strongly"
> and "weakly" variations. The authors can modify the random forcing
> term to achieve higher Reynolds.

We have now replaced "strongly" and "weakly" in the various places
in the manuscript by more precise statements by writing:
that \sigma_A is proportional to Re_lambda to the 3/2 power, but only
proportional to \bar{\epsilon} to the -1/5 power.

>- -Page 1/l. 11: the simulations have been done without updraft. The authors should
> add a paragraph in the introduction of the effects and consequences of the updraft
> in the broadening of droplet size distributions.

We have now added the following discussion at the end of the second
paragraph of section 1 on page 2: "When the mean updraft velocity is not
zero, there could be a competition between the mean updraft velocity and
supersaturation fluctuations. This may diminish the role of supersaturation
fluctuations (Sardina et al. 2018)."

> -Page 2/l. 17: Paoli Sharif results are strongly influenced by an
> arbitrary forcing term for the temperature and water vapor equations

We have now addressed the "arbitrary forcing term" by saying
"turbulence as well as stochastically forced temperature and vapor".

> -Page 2/l. 26-27 (and many other locations in the manuscript): Can the
> authors comment on the sentence "solve the thermodynamics" when the
> maximum temperature fluctuations of their system are 0.1 K?

The main difference between the present study and that of Sardina et al.
is that we solve the supersaturation explicitly by solving the
temperature and water vapor mixing ratio field. This is why we say
that we "solve for the temperature field". Due to the limited Reynolds
number in DNS, the temperature fluctuations are small. In this sense,
it is indeed acceptable to treat the supersaturation as a passive
scalar. Nevertheless, solving for the temperature and water vapor mixing
ratio directly is beneficial when one wants to incorporate entrainment
and so on, which is an ongoing project.

> -Page 3/l. 8: Can the authors provide a plot with the ratio between a_{rms} and B_{r
ms}
> where a is the fluid acceleration (the material derivative of the velocity)?
> My feeling is that at these small scales buoyancy effects can be neglected.

The forced turbulence becomes stationary.
In this case, a_{rms}/B_{rms}=250.
Therefore, the buoyancy force is indeed small.
We have now discussed this in the last paragraph of page 8.
The figure showing a_{rms}/B_{rms} is attached as
supplementary material.

> -Page 3/l. 31: A theoretical issue: the velocity field within the
> Boussinesq approximation is divergence free that is not the case. A short
> paragraph should be added to justify this theoretical mismatch briefly.

We discussed that "The background air flow is almost incompressible and

thus obeys the Boussinesq approximation." in the first paragraph of
section 2.1.

> -Page 8/l. 5: How can you see that equation 18 follows a Brownian motion?

We have now changed it to the following, "It can be seen from \Eq{eq:A}
that the evolution of the surface area is analogy to Brownian motion,"
at P.10/l.3.

> -Page 11/l.15: ¿Therefore, neglecting the smallest scales in the stochastic model is
> indeed acceptable¿, the stochastic models are derived under the hypothesis of large-
> scale separation so that they cannot be applied at Re ¿ = 40. If you want to show sl
ightly
> less dependence repeat the same simulation set up with three different dissipation f
or
> the higher resolution setup.

We have now updated all the figures for different \epsilon with Re_lambmda=130.

> -Page 12/l.3: I guess that the contradiction is due to the presence of updraft

We have now added the following discussion at P.14/l.1-2,
"It could also be due to the mean updraft
cooling included in the model of Vaillancourt et al. (2002), which
was excluded in the present study and in the work of others."

> -The three appendices containing just one definition are not needed, please move in
> main text

We have now moved all the appendix to the
main text.

> Technical corrections:
> -Pag3 3/l.13: is to are

We have now corrected it.

> -Page 3/l.22: there is a 0 after the citation Li et al, 2017

We have now corrected it.

> -Page 3/l.29: provide a reference for the code

We provided it in the last sentence of the acknowledgement.

> -Page 4/l.11: index and vectorial notations should not be mixed

We have now only adopted the tensor notation.

> -Page 6/l.5: is the nonlinear correction needed? What is the range of droplet Reynol
ds
> number?

It is between 3 to 5.5, which is almost negligible. Nevertheless,
we always turn this on so that collision-coalescence can be
investigated as a sequential work.

> -Page 6/l.25: I guess the factor 2 \beta is wrong, otherwise, it would be 2 64 for t
he larger
> case!!!

We have now removed the statement because \beta is not used elsewhere in the manuscrip
t.

> -Page 6: there is no need to create a new subsection 3.2

Section 3.2 is the DNS, which is to be distinguished from the initial
configuration in 3.1.

> -Page 7/l.7: fix Kolmogorov

We have now fixed it,

Anonymous Referee #2
Received and published: 16 October 2018

> The focus of this paper is the influence of supersaturation fluctuations
> on droplet condensation growth, which has become an active area of
> research in recent years. To have the stratiform clouds as a motivation,
> authors have studied this effect in the absence of the mean updraft
> velocity. In this study, the conservation of momentum and scalar
> (temperature and water vapor) equations are solved using the direct
> numerical simulation (DNS) in a rectangular domain and the random
> velocity forcing drives the turbulence. Here, the Eulerian scalar and
> momentum field is coupled with the Lagrangian droplet dynamics using the
> superparticle method. Additionally, the physics of droplet activation
> and droplet collision-coalescence process were ignored. All droplets were
> considered at an initial size of 10 um and the starting supersaturation
> in the domain was 2%. Authors have examined cases of different Taylor
> Reynolds number (Re_\lambda) and mean kinetic energy dissipation rate (\bar{\epsilon
}).
> In general, the approach here is very much similar to that of Sardina
> et al. (2015), Siewert at al. (2017) and others. The only significant
> difference is the treatment of supersaturation field; in the current
> case, it is obtained by solving temperature and water vapor conservation
> equations contrary to the assumption of supersaturation field as a
> passive scalar in previous studies. Moreover, the authors compared the
> results with the stochastic formulation of Sardina et al. (2015) and other
> numerical-simulation studies. The results are consistent with the other
> studies, the droplet size dispersion (\sigma_A) growth is proportional to
> t^1/2. Similarly, the broadening in droplet size distribution is shown
> to be nearly independent of (a slight decrease), however, it increases
> with increase in Re_\lambda consistent with the conclusions of Sardina et
> al. (2015).

We thank the reviewer for his/her constructive comments and have now emphasized
the novelty of our work in various places. Our detailed response to the
reviewer's comments are explained below, highlighted in blue.

> Review points:
> - The authors should be clear about the novelty. The main significant
> differences between current simulation and previous are the treatment of
> supersaturation field and the feedback due to condensation. Although,
> authors also acknowledge that the treatment of supersaturation as a
> passive scalar is sufficient. Furthermore, they explicitly showed that
> the results are independent to the dissipation rate () which was not
> clearly presented in the other studies. Please update abstract, intro
> and conclusions to make clear.

We have now added the following in:
1. abstract
"The supersaturation field is calculated directly by
simulating the temperature and water vapor fields instead
of treating it as a passive scalar. Thermodynamic feedbacks
to the fields due to condensation are also included."

"Also, for the first time, we explicitly demonstrate that the time evolution of the si
ze distribution..."

2. introduction
We addressed that
P.2/l.29-30: "Neither Sardina et al. (2015) nor Siewert et al. (2017)
solved the thermodynamics that determine the supersaturation field."
P.3/l.11-12: "where turbulence, thermodynamics,
feedback from droplets to the fields via the condensation rate
and buoyancy force are all included."
P.3/l.15-17: "For the first time, to our knowledge,

the stochastic model and simulation results from
the complete set of equations governing the supersaturation field is compared."

3. conclusion
P13/l5-6: "For the first time, we explicitly demonstrate that the size distribution be
comes wider
with increasing Re_lambda, which is, however, insensitive to \bar{\epsilon}."

> - Claimed relevance is to stratocumulus clouds, but entrainment of unsaturated air a
nd
> possible secondary activation is know to strongly change droplet size distribution i
n that
> system. How does absence of entrainment limit the results presented? What changes
> can be expected when entrainment and activation are included? These limitations
> should be discussed.

We have now added the following:
P.14/10-13: "Entrainment of dry air is not considered here, which may
lead to very rapid changes of supersaturation fluctuations
and result in fast broadening of the size distribution Kumar et al. (2014).
Activation of aerosols in a turbulent environment is omitted.
This may provide a more physical and realistic initial distribution of cloud droplets.
Incorporating all the cloud microphysical processes is computationally
challenging, which will be explored further in the future studies."

> - Page-6, Line 16: It should be supersaturation instead of saturation.

We have now corrected it.

> - Page-7, Line 7: Fix the typo

We have now fixed it.

> - The assumption used to get the eq. 20 is not required to derive the equation for \
sigma_A growth.

The scaling law \sigma_A~t^{1/2} does not require the assumption.
However, to obtain eq.23, T_0>>\tau_phase is needed.
We have now added the explanation below eq 22 on page 10.

> - The phase relaxation time might be changing with time due to the mean radius growt
h
> (specifically, at the starting since there is a starting supersaturation around 2%).
 It
> might cause some deviation in the result (\sigma_A vs t) from the t 1/2 relation. Au
thors should
> discuss this effect along with the discussion of figure 4.

We have now added a discussion in the last paragraph at P.12/l.9-12.

Cloud-droplet growth due to supersaturation fluctuations in stratiform clouds

Xiang-Yu Li[1,2,3,4,5], Gunilla Svensson[1,3,6], Axel Brandenburg[2,4,5,7], and Nils E. L. Haugen[8,9]

[1]Department of Meteorology and Bolin Centre for Climate Research, Stockholm University, Stockholm, Sweden
[2]Nordita, KTH Royal Institute of Technology and Stockholm University, 10691 Stockholm, Sweden
[3]Swedish e-Science Research Centre, www.e-science.se, Stockholm, Sweden
[4]Laboratory for Atmospheric and Space Physics, University of Colorado, Boulder, CO 80303, USA
[5]JILA, Box 440, University of Colorado, Boulder, CO 80303, USA
[6]Global & Climate Dynamics, National Center for Atmospheric Research, Boulder, CO 80305, USA
[7]Department of Astronomy, Stockholm University, SE-10691 Stockholm, Sweden
[8]SINTEF Energy Research, 7465 Trondheim, Norway
[9]Department of Energy and Process Engineering, NTNU, 7491 Trondheim, Norway

Correspondence: Xiang-Yu Li (xiang.yu.li@su.se), November 3, 2018, Revision: 1.189

Abstract.

Condensational growth of cloud droplets due to supersaturation fluctuations is investigated by solving the hydrodynamic and thermodynamic equations using direct numerical simulations with droplets being modeled as Lagrangian particles. The supersaturation field is calculated directly by simulating the temperature and water vapor fields instead of being treated as a passive scalar. Thermodynamic feedbacks to the fields due to condensation are also included for completeness. We find that the width of droplet size distributions increases with time, which is contrary to the classical theory without supersaturation fluctuations, where condensational growth leads to progressively narrower size distributions. Nevertheless, in agreement with earlier Lagrangian stochastic models of the condensational growth, the standard deviation of the surface area of droplets increases as $t^{1/2}$. Also, for the first time, we explicitly demonstrate that the time evolution of the size distribution is sensitive to the Reynolds number, but insensitive to the mean energy dissipation rate. This is shown to be due to the fact that temperature fluctuations and water vapor mixing ratio fluctuations increases with increasing Reynolds number, therefore the resulting supersaturation fluctuations are enhanced with increasing Reynolds number. Our simulations may explain the broadening of the size distribution in stratiform clouds qualitatively, where the mean updraft velocity is almost zero.

1 Introduction

The growth of cloud droplets is dominated by two processes: condensation and collection. Condensation of water vapor on active cloud condensation nuclei is important in the size range from the activation size of aerosol particles to about a radius of $10\,\mu\mathrm{m}$ (Pruppacher and Klett, 2012; Lamb and Verlinde, 2011). Since the rate of droplet growth by condensation is inversely proportional to the droplet radius, large droplets grow slower than smaller ones. This generates narrower size distributions (Lamb and Verlinde, 2011). To form rain droplets in warm clouds, small droplets must grow to about $50\,\mu\mathrm{m}$ in radius within

15–20 minutes (Pruppacher and Klett, 2012; Devenish et al., 2012; Grabowski and Wang, 2013; Seinfeld and Pandis, 2016). Therefore, collection, a widely accepted microscopical mechanism, has been proposed to explain the rapid formation of rain droplets (Saffman and Turner, 1956; Berry and Reinhardt, 1974; Shaw, 2003; Grabowski and Wang, 2013). However, collection can only become active when the size distribution reaches a certain width.

Hudson and Svensson (1995) observed a broadening of the droplet size distribution in Californian marine stratus, which was contrary to the classical theory of condensational growth (Yau and Rogers, 1996). The increasing width of droplet size distributions were further observed by Pawlowska et al. (2006) and Siebert and Shaw (2017b). The contradiction between the observed broadening width and the theoretical narrowing width in the absence of turbulence has stimulated several studies. The classical treatment of diffusion-limited growth assumes that supersaturation depends only on average temperature and water mixing ratio. Since fluctuations of temperature and the water mixing ratio are affected by turbulence, the supersaturation fluctuations are inevitably subjected to turbulence. Naturally, condensational growth due to supersaturation fluctuations became the focus (Srivastava, 1989; Korolev, 1995; Sardina et al., 2015; Siewert et al., 2017; Grabowski and Abade, 2017). The supersaturation fluctuations are particularly important for understanding the condensational growth of cloud droplets in stratiform clouds, where the updraft velocity of the parcel is almost zero (Hudson and Svensson, 1995; Korolev, 1995). When the mean updraft velocity is not zero, there could be a competition between mean updraft velocity and supersaturation fluctuations. This may diminish the role of supersaturation fluctuations (Sardina et al., 2018).

Condensational growth due to supersaturation fluctuations was first recognized by Srivastava (1989), who criticized the use of a volume-averaged supersaturation and proposed a randomly distributed supersaturation field. Using direct numerical simulations (DNS), Vaillancourt et al. (2002) found that turbulence has negligible effect on condensational growth and attributed this to the decorrelation between the supersaturation and the droplet size. Paoli and Shariff (2009) considered three-dimensional (3-D) turbulence as well as stochastically forced temperature and vapor fields with a focus on statistical modeling for large-eddy simulations. They found that supersaturation fluctuations are responsible for the broadening of the droplet size distribution, which is contrary to the findings by Vaillancourt et al. (2002). Lanotte et al. (2009) conducted 3-D DNS for condensational growth by only solving a passive scalar equation for the supersaturation and concluded that the width of the size distribution increases with increasing Reynolds number. Sardina et al. (2015) extended the DNS of Lanotte et al. (2009) to higher Reynolds number and found that the variance of the size distribution increases in time. In a similar manner as Sardina et al. (2015), Siewert et al. (2017) modelled the supersaturation field as a passive scalar coupled to the Lagrangian particles and found that their results can be reconciled with those of earlier numerical studies by noting that the droplet size distribution broadens with increasing Reynolds number (Paoli and Shariff, 2009; Lanotte et al., 2009; Sardina et al., 2015). Neither Sardina et al. (2015) nor Siewert et al. (2017) solved the thermodynamics that determine the supersaturation field. Both Saito and Gotoh (2017) and Chen et al. (2018) solved the thermodynamics equations governing the supersaturation field. However, since collection was also included in their work, one cannot clearly identify the roles of turbulence on collection or condensational growth, nor can one compare their results with Lagrangian stochastic models (Sardina et al., 2015; Siewert et al., 2017) related to condensational growth. Grabowski and Wang (2013) proposed the eddy-hopping mechanism to explain the broadening and investigated it in Grabowski and Abade (2017).

Recent laboratory experiments and observations about cloud microphysics also confirm the notion that supersaturation fluctuations may play an important role in broadening the size distribution of cloud droplets. The laboratory study by Chandrakar et al. (2016) suggested that supersaturation fluctuations in the low aerosol number concentration limit are likely of leading importance for precipitation formation. The condensational growth due to supersaturation fluctuations seems to be more sensitive to the integral scale of turbulence (Götzfried et al., 2017). Siebert and Shaw (2017a) measured the variability of temperature, water vapor mixing ratio, and supersaturation in warm clouds and support the notion that both aerosol particle activation and droplet growth take place in the presence of a broad distribution of supersaturation (Hudson and Svensson, 1995; Brenguier et al., 1998; Miles et al., 2000; Pawlowska et al., 2006). The challenge is now how to interpret the observed broadening of droplet size distribution in warm clouds. How does turbulence drive fluctuations of the scalar fields (temperature and water vapor mixing ratio) and therefore affect the broadening of droplet size distributions (Siebert and Shaw, 2017a)?

In an attempt to answer this question, we conduct 3-D DNS experiments of condensational growth of cloud droplets, where turbulence, thermodynamics, feedback from droplets to the fields via the condensation rate and buoyancy force are all included. The main aim is to investigate how supersaturation fluctuations affect the droplet size distribution. We particularly focus on the time evolution of the size distribution $f(r,t)$ and its dependency on small and large scales of turbulence. We then compare our simulation results with Lagrangian stochastic models (Sardina et al., 2015; Siewert et al., 2017). For the first time, the stochastic model and simulation results from the complete set of equations governing the supersaturation field are compared.

2 Numerical model

We now discuss the basic equations where we combine the Eulerian description of the density (ρ), turbulent velocity ($\boldsymbol{u}$), temperature (T), and water vapor mixing ratio (q_v) with the Lagrangian description of the ensemble of cloud droplets. The water vapor mixing ratio q_v is defined as the ratio between the mass density of water vapor and dry air. Droplets are treated as superparticles. A superparticle represents an ensemble of droplets, whose mass, radius, and velocity are the same as those of each individual droplet within it (Shima et al., 2009; Johansen et al., 2012; Li et al., 2017). For condensational growth, the superparticle approach (Li et al., 2017) is the same as the Lagrangian point-particle approach (Kumar et al., 2014) since there is no interactions among droplets. Nevertheless, we still use the superparticle approach so that we can include more processes like collection (Li et al., 2017, 2018) in future. Another reason to adopt superparticle approach is that it can be easily adapted to conduct Large-eddy simulations with appropriate sub-grid scale models (Grabowski and Abade, 2017). To investigate the condensational growth of cloud droplets that experience fluctuating supersaturation, we track each individual superparticle in a Lagrangian manner. The motion of each superparticle is governed by the momentum equation for inertial particles. The supersaturation field in the simulation domain is determined by $T(\boldsymbol{x},t)$ and $q_v(\boldsymbol{x},t)$ transported by turbulence. Lagrangian droplets are exposed in different supersaturation fields. Therefore, droplets either grow by condensation or shrink by evaporation depending on the local supersaturation field. This phase transition generates a buoyancy force, which in turn affects the turbulent kinetic energy, $T(\boldsymbol{x},t)$, and $q_v(\boldsymbol{x},t)$. PENCIL CODE is used to conduct all the simulations.

2.1 Equations of motion for Eulerian fields

The background air flow is almost incompressible and thus obeys the Boussinesq approximation. Its density $\rho(\boldsymbol{x},t)$ is governed by the continuity equation and velocity $\boldsymbol{u}(\boldsymbol{x},t)$ by Navier-Stokes equation. The temperature $T(\boldsymbol{x},t)$ of the background air flow is determined by the energy equation with a source term due to the latent heat release. The water vapor mixing ratio $q_v(\boldsymbol{x},t)$ is transported by the background air flow. The Eulerian equations are given by

$$\frac{\partial\rho}{\partial t}+\boldsymbol{\nabla}\cdot(\rho\boldsymbol{u})=S_\rho, \tag{1}$$

$$\frac{D\boldsymbol{u}}{Dt}=\boldsymbol{f}-\rho^{-1}\boldsymbol{\nabla}p+\rho^{-1}\boldsymbol{\nabla}\cdot(2\nu\rho\mathsf{S})+B\boldsymbol{e}_z+\boldsymbol{S}_u, \tag{2}$$

$$\frac{DT}{Dt}=\kappa\nabla^2T+\frac{L}{c_p}C_d, \tag{3}$$

$$\frac{Dq_v}{Dt}=D\nabla^2q_v-C_d, \tag{4}$$

where $D/Dt=\partial/\partial t+\boldsymbol{u}\cdot\boldsymbol{\nabla}$ is the material derivative, $\boldsymbol{f}$ is a random forcing function (Haugen et al., 2004), ν is the kinematic viscosity of air, $\mathsf{S}_{ij}=\frac{1}{2}(\partial_j u_i+\partial_i u_j)-\frac{1}{3}\delta_{ij}(\partial_k u_k)$ is the traceless rate-of-strain tensor, p is the gas pressure, ρ is the gas density, c_p is the specific heat at constant pressure, L is the latent heat, κ is the thermal diffusivity of air, C_d is the condensation rate, B is the buoyancy, e_z is the unit vector in the z direction (vertical direction), and D is the diffusivity of water vapor. To avoid global transpose operations associated with calculating Fourier transforms for solving the nonlocal equation for the pressure in strictly incompressible calculations, we solve here instead the compressible Navier-Stokes equations using high-order finite differences. The sound speed c_s obeys $c_\mathrm{s}^2=\gamma p/\rho$, where $\gamma=c_\mathrm{p}/c_\mathrm{v}=7/5$ is the ratio between specific heats, c_p and c_v, at constant pressure and constant volume, respectively. We set the sound speed as $5\,\mathrm{m\,s^{-1}}$ to simulate the nearly incompressible atmospheric air flow, resulting in a Mach number of 0.06 when $u_\mathrm{rms}=0.27\,\mathrm{m\,s^{-1}}$, where u_rms is the rms velocity. Such a configuration, with so small Mach number, is almost equivalent to an incompressible flow. It is worth noting that the temperature determining the compressibility of the flow is constant and independent of the temperature field of the gas flow governed by Equation (3). Also, since the gas flow is almost incompressible and its mass density is much smaller than the one of the droplet, there is no mass exchange between the gas flow and the droplet, i.e., the density of the gas flow $\rho(\boldsymbol{x},t)$ is not affected by $T(\boldsymbol{x},t)$. Thus, the source terms S_ρ and $\boldsymbol{S}_u$ in Equations (1) and (2) are neglected (Krüger et al., 2017). The buoyancy $B(\boldsymbol{x},t)$ depends on the temperature $T(\boldsymbol{x},t)$, water vapor mixing ratio $q_v(\boldsymbol{x},t)$, and the liquid mixing ratio q_l (Kumar et al., 2014),

$$B(\boldsymbol{x},t)=g(T'/T+\alpha q_v'-q_l), \tag{5}$$

where $\alpha=M_a/M_v-1\approx 0.608$ when M_a and M_v are the molar masses of air and water vapor, respectively. The amplitude of the gravitational acceleration is given by g. The liquid water mixing ratio is the ratio between the mass density of liquid water and the dry air and is defined as

$$q_l(\boldsymbol{x},t) = \frac{4\pi\rho_l}{3\rho_a(\Delta x)^3}\sum_{j=1}^{N_\triangle} r(t)^3 = \frac{4\pi\rho_l}{3\rho_a}\sum_{j=1}^{N_\triangle} f(r,t) r(t)^3\,\delta r, \tag{6}$$

where ρ_l and ρ_a are the liquid water density and the reference mass density of dry air. $N_\triangle$ is the total number of droplets in a cubic grid cell with volume $(\Delta x)^3$, where Δx is the one-dimensional size of the grid box. The temperature fluctuations are given by

$$T'(\boldsymbol{x},t) = T(\boldsymbol{x},t) - T_{\mathrm{env}}, \tag{7}$$

and the water vapor mixing ratio fluctuations by

$$q_v'(\boldsymbol{x},t) = q_v(\boldsymbol{x},t) - q_{v,\mathrm{env}}. \tag{8}$$

We adopt the same method as in Kumar et al. (2014), where the mean environmental temperature T_{env} and water vapor mixing ratio $q_{v,\mathrm{env}}$ do not change in time. This assumption is plausible in the circumstance that we do not consider the entrainment, i.e., there is only mass and energy transfer between liquid water and water vapor. The condensation rate C_d (Vaillancourt et al., 2001) is given by

$$C_d(\boldsymbol{x},t) = \frac{4\pi\rho_l G}{\rho_a(\Delta x)^3}\sum_{j=1}^{N_\triangle} s(\boldsymbol{x},t) r(t) = \frac{4\pi\rho_l G}{\rho_a}\sum_{j=1}^{N_\triangle} s(\boldsymbol{x},t) f(\boldsymbol{x},t) r(t)\,\delta r, \tag{9}$$

where G is the condensation parameter (in units of $\mathrm{m^2\,s^{-1}}$), which depends weakly on temperature and pressure and is here assumed to be constant (Lamb and Verlinde, 2011). The supersaturation s is defined as the ratio between the vapor pressure e_v and the saturation vapor pressure e_s,

$$s = \frac{e_v}{e_s} - 1. \tag{10}$$

Using the ideal gas law, Equation (10) can be expressed as,

$$s = \frac{\rho_v R_v T}{\rho_{vs} R_v T} - 1 = \frac{\rho_v}{\rho_{vs}} - 1. \tag{11}$$

In terms of the water vapor mixing ratio $q_v = \rho_v/\rho_a$ and saturation water vapor mixing ratio $q_{vs} = \rho_{vs}/\rho_a$, Equation (11) can be written as:

$$s(\boldsymbol{x},t) = \frac{q_v(\boldsymbol{x},t)}{q_{vs}(T)} - 1. \tag{12}$$

Here ρ_v is the mass density of water vapor and ρ_{vs} the mass density of saturated water vapor, and $q_{vs}(T)$ is the saturation water vapor mixing ratio at temperature T and can be determined by the ideal gas law,

$$q_{vs}(T) = \frac{e_s(T)}{R_v \rho_a T}. \tag{13}$$

The saturation vapor pressure e_s over liquid water is the partial pressure due to the water vapor when an equilibrium state of evaporation and condensation is reached for a given temperature. It can be determined by the Clausius-Clapeyron equation, which determines the change of e_s with temperature T. Assuming constant latent heat L, e_s is approximated as (Yau and Rogers, 1996; Götzfried et al., 2017)

$$e_s(T) = c_1 \exp(-c_2/T), \tag{14}$$

where c_1 and c_2 are constants adopted from page 14 of Yau and Rogers (1996). We refer to Table 1 for all the thermodynamics constants. In the present study, the updraft cooling is omitted. Therefore, the assumption of constant latent heat L is plausible.

2.2 Lagrangian model for cloud droplets

In addition to the Eulerian fields described in Section 2.1 we treat cloud droplets as Lagrangian particles. In the PENCIL CODE, they are invoked as non-interacting superparticles.

2.2.1 Kinetics of cloud droplets

Each superparticle is treated as a Lagrangian point-particle, where one solves for the particle position $\boldsymbol{x}_i$,

$$\frac{d\boldsymbol{x}_i}{dt} = \boldsymbol{V}_i, \tag{15}$$

and its velocity $\boldsymbol{V}_i$ via

$$\frac{d\boldsymbol{V}_i}{dt} = \frac{1}{\tau_i}(\boldsymbol{u} - \boldsymbol{V}_i) + g\boldsymbol{e}_z, \tag{16}$$

in the usual way; see (Li et al., 2017) for details. Here, $\boldsymbol{u}$ is the fluid velocity at the position of the superparticle, τ_i is the particle inertial response or stopping time of a droplet i and is given by

$$\tau_i = 2\rho_l r_i^2/[9\rho\nu\, D(\mathrm{Re}_i)]. \tag{17}$$

The correction factor (Schiller and Naumann, 1933; Marchioli et al., 2008),

$$D(\mathrm{Re}_i) = 1 + 0.15\,\mathrm{Re}_i^{2/3}, \tag{18}$$

models the effect of non-zero particle Reynolds number $\mathrm{Re}_i = 2r_i|\boldsymbol{u} - \boldsymbol{V}_i|/\nu$. This is a widely used approximation, although it does not correctly reproduce the small-$\mathrm{Re_i}$ correction to Stokes formula (Veysey and Goldenfeld, 2007).

2.2.2 Condensational growth of cloud droplets

The condensational growth of the particle radius r_i is governed by (Pruppacher and Klett, 2012; Lamb and Verlinde, 2011)

$$\frac{\mathrm{d}r_i}{\mathrm{d}t} = \frac{Gs\,(\boldsymbol{x}_i, t)}{r_i}. \tag{19}$$

3 Experimental setup

3.1 Initial configurations

The initial values of the water vapor mixing ratio $q_v(\boldsymbol{x}, t=0) = 0.0157\,\mathrm{kg} \cdot \mathrm{kg}^{-1}$ and temperature $T(\boldsymbol{x}, t=0) = 292\,\mathrm{K}$ are matched to the ones obtained in the CARRIBA experiments (Katzwinkel et al., 2014), which are the same as those in Götzfried et al. (2017). With this configuration, we obtain $s(\boldsymbol{x}, t=0) = 2\%$, which means that the water vapor is initially supersaturated. The time step of the simulations presented here is governed by the smallest time scale in the present configuration, which is the particle stopping time defined in Equation (17). The thermodynamic time scale is much larger than the turbulent one. Table 1 shows the list of thermodynamic parameters used in the present study.

Initially, 10 μm-sized droplets with zero velocity are randomly distributed in the simulation domain. The mean number density of droplets, which is constant in time since droplet collections are not considered, is $n_0 = 2.5 \times 10^8\,\mathrm{m}^{-3}$. This gives an initial liquid water content, $\int_0^\infty f(r, t=0)\, r^3\, \mathrm{d}r$, which is $0.001\,\mathrm{kg\,m}^{-3}$. The simulation domain is a cube of size $L_x = L_y = L_z$, the values of which are given in Table 2. The number of superparticles N_s satisfies $N_\mathrm{s}/N_\mathrm{grid} \approx 0.1$, where N_grid is the number of lattices depending on the spatial resolution of the simulations. Setting $N_\mathrm{s}/N_\mathrm{grid} \approx 0.1$, on one hand, is still within the convergence range $N_\mathrm{s}/N_\mathrm{grid} \approx 0.05$ (Li et al., 2018). On the other hand, it can mimic the diluteness of the atmospheric cloud system, where there are about 0.1 droplets per cubic Kolmogorov scale. This configuration results in $N_{\mathrm{s},128} = 244140$ when $N_\mathrm{grid} = 128^3$.

3.2 DNS

We conduct high resolution simulations for different Taylor micro-scale Reynolds number Re_λ and mean energy dissipation rate $\bar{\epsilon}$ (see Table 2 for details of the simulations). The Taylor micro-scale Reynolds number is defined as $\mathrm{Re}_\lambda \equiv u_\mathrm{rms}^2 \sqrt{5/(3\nu\bar{\epsilon})}$. For simulations with different values of $\bar{\epsilon}$ at fixed Re_λ, we vary both the domain size L_x ($L_y = L_z = L_x$) and the amplitude of the forcing f_0. As for fixed $\bar{\epsilon}$, Re_λ is varied by solely changing the domain size, which in turn changes u_rms. In all simulations, we use for the Prandtl number $\mathrm{Pr} = \nu/\kappa = 1$ and for the Schmidt number $Sc = \nu/D = 0.6$. For our simulations with $N_\mathrm{grid} = 512^3$ meshpoints, the code computes 55,000 time steps in 24 hours wall-clock time using 4096 cores. For $N_\mathrm{grid} = 128^3$ meshpoints, the code computes 4.5 million time steps in 24 hours wall-clock time using 512 cores.

4 Results

Figure 1(a) shows time-averaged turbulent kinetic-energy spectra for different values of $\bar{\epsilon}$ at fixed $\mathrm{Re}_\lambda \approx 130$. Since the abscissa in the figures is normalized by $k_\eta = 2\pi/\eta$, the different spectra shown in Figure 1(a) collapse onto a single curve. Here, η is the Kolmogorov length scale. Figure 1(b) shows the time-averaged turbulent kinetic-energy spectra for different values of Re_λ at fixed $\bar{\epsilon} \approx 0.039\,\mathrm{m^2 s^{-3}}$. For larger Reynolds numbers the spectra extend to smaller wavenumbers. A flat profile corresponds to Kolmogorov scaling (Pope, 2000) when the energy spectrum is compensated by $\bar{\epsilon}^{-2/3} k^{5/3}$. For the largest Re_λ in our simulations ($\mathrm{Re}_\lambda = 130$), the inertial range extends for about a decade in k-space.

Table 1. List of constants for the thermodynamics: see text for explanations of symbols.

Quantity	Value
$\nu\,(\mathrm{m^2\,s^{-1}})$	1.5×10^{-5}
$\kappa\,(\mathrm{m^2\,s^{-1}})$	1.5×10^{-5}
$D\,(\mathrm{m^2\,s^{-1}})$	2.55×10^{-5}
$G\,(\mathrm{m^2\,s^{-1}})$	1.17×10^{-10}
c_1 (Pa)	2.53×10^{11}
c_2 (K)	5420
$L\,(\mathrm{J\cdot kg^{-1}})$	2.5×10^{6}
$c_\mathrm{p}\,(\mathrm{J\cdot kg^{-1}K^{-1}})$	1005.0
$R_v\,(\mathrm{J\cdot kg^{-1}K^{-1}})$	461.5
$M_a\,(\mathrm{g\cdot mol^{-1}})$	28.97
$M_v\,(\mathrm{g\cdot mol^{-1}})$	18.02
$\rho_a\,(\mathrm{kg\cdot m^{-3}})$	1
$\rho_l\,(\mathrm{kg\cdot m^{-3}})$	1000
α	0.608
$\mathrm{Pr}=\nu/\kappa$	1
$Sc=\nu/D$	0.6
$q_v(\boldsymbol{x},t=0)\,(\mathrm{kg\cdot kg^{-1}})$	0.0157
$q_{v,\mathrm{env}}\,(\mathrm{kg\cdot kg^{-1}})$	0.01
$T(\boldsymbol{x},t=0)\,(\mathrm{K})$	292
$T_\mathrm{env}\,(\mathrm{K})$	293

Table 2. Summary of the simulations; see text for explanation of symbols.

Run	f_0	$L_x\,(\mathrm{m})$	N_grid	N_s	$u_\mathrm{rms}\,(\mathrm{m\,s^{-1}})$	Re_λ	$\bar\epsilon\,(\mathrm{m^2s^{-3}})$	$\eta\cdot10^{-4}\,(\mathrm{m})$	τ_η (s)	τ_L (s)	τ_s (s)	Da
A	0.02	0.125	128^3	$N_{\mathrm{s},128}$	0.16	45	0.039	5.4	0.020	0.25	0.014	0.053
B	0.02	0.25	256^3	$2^3N_{\mathrm{s},128}$	0.22	78	0.039	5.4	0.020	0.37	0.014	0.081
C	0.02	0.5	512^3	$2^6N_{\mathrm{s},128}$	0.28	130	0.039	5.4	0.020	0.58	0.014	0.125
D	0.014	0.6	512^3	$2^6N_{\mathrm{s},128}$	0.24	135	0.019	6.5	0.028	0.81	0.014	0.174
E	0.007	0.8	512^3	$2^6N_{\mathrm{s},128}$	0.17	138	0.005	8.9	0.053	1.47	0.014	0.312

Next we inspect the response of thermodynamics to turbulence. In Figure 2, we show time series of fluctuations of temperature T_rms, water vapor mixing ratio $q_{v,\mathrm{rms}}$, buoyancy force B_rms, and the supersaturation s_rms. All quantities reach a statistically steady state within a few seconds. The steady state values of T_rms, $q_{v,\mathrm{rms}}$, and s_rms increase with increasing Re_λ approximately linearly, and vary hardly at all with $\bar\epsilon$. On the other hand. B_rms changes only by a few percent as Re_λ or $\bar\epsilon$ vary.

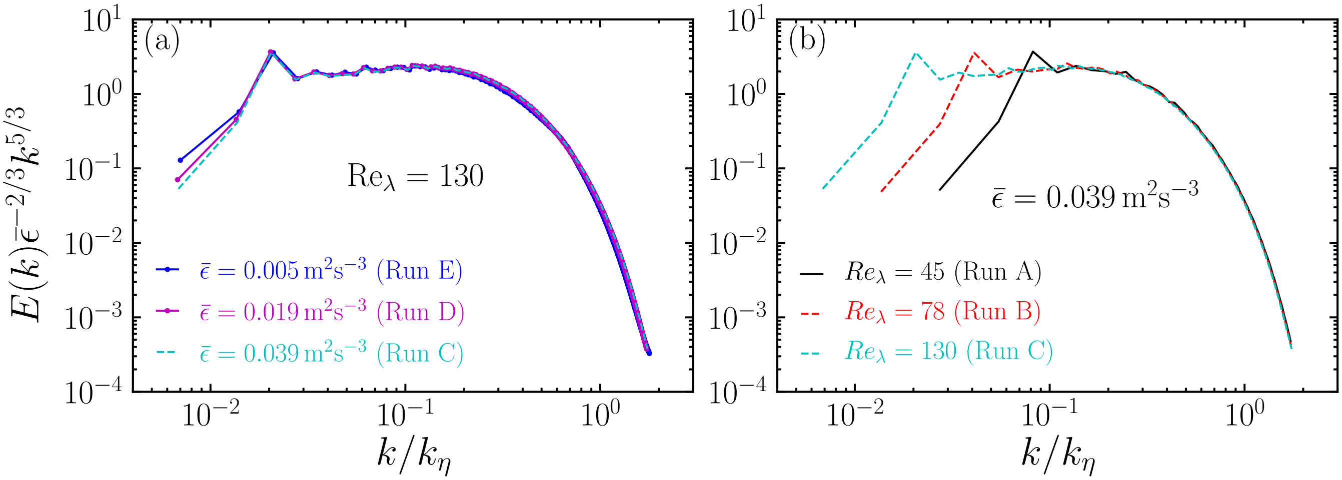

Figure 1. Time-averaged kinetic energy spectra of the turbulence gas flow for (a) different $\bar{\epsilon} = 0.005\,\mathrm{m^2s^{-3}}$ (blue dash-dotted line), 0.019 (magenta dash-dotted line) and 0.039 (black solid line) at fixed $\mathrm{Re}_\lambda = 130$ (see Runs C, D, and E in Table 2 for details) and for (b) different $\mathrm{Re}_\lambda = 45$ (black solid line), 78 (red dashed line), and 130 (cyan dashed line) at fixed $\bar{\epsilon} = 0.039\mathrm{m^2s^{-3}}$ (see Runs A, B, and C in Table 2 for details).

Note, however, that the buoyancy force is only about 0.3% of the fluid acceleration. This is because T_{rms} is small (about $0.1\,\mathrm{K}$ in the present study). Therefore, the effect of the buoyancy force should indeed be small.

When changing $\bar{\epsilon}$ while keeping Re_λ fixed, the Kolmogorov scales of turbulence varies. Therefore, the various fluctuations quoted above are insensitive to the small scales of turbulence. However, when varying Re_λ while keeping $\bar{\epsilon}$ fixed, their rms values change, which is due to large scales of turbulence. Indeed, temperature fluctuations are driven by the large scales of turbulence, which affects the supersaturated vapor pressure q_{vs} via the Clausius-Clapeyron equation; see Equation (13). Therefore, supersaturation fluctuations result from both temperature fluctuations and water vapor fluctuations via Equation (12). Both $q_{v,\mathrm{rms}}$ and T_{rms} increase with increasing Re_λ, resulting in larger fluctuations of s. Supersaturation fluctuations, in turn, affect T and q_v via the condensation rate C_d.

Our goal is to investigate the condensational growth of cloud droplets due to supersaturation fluctuations. Figure 3 shows the time evolution of droplet size distributions for different configurations. The conventional understanding is that condensational growth leads to a narrow size distribution (Pruppacher and Klett, 2012; Lamb and Verlinde, 2011). However, supersaturation fluctuations broaden the distribution. More importantly, the width of the size distribution increases with increasing Re_λ, but *decreases* slightly with increasing $\bar{\epsilon}$ over the range studied here. This is consistent with the results shown in Figure 2 in that supersaturation fluctuations are sensitive to Re_λ but are insensitive to $\bar{\epsilon}$. In atmospheric clouds, $\mathrm{Re}_\lambda \approx 10^4$, which may result in an even broader size distribution.

We further quantify the variance of the size distribution by investigating the time evolution of the standard deviation of the droplet surface area σ_A for different configurations. In terms of the droplet surface area A_i ($A_i \propto r_i^2$), Equation (19) can be

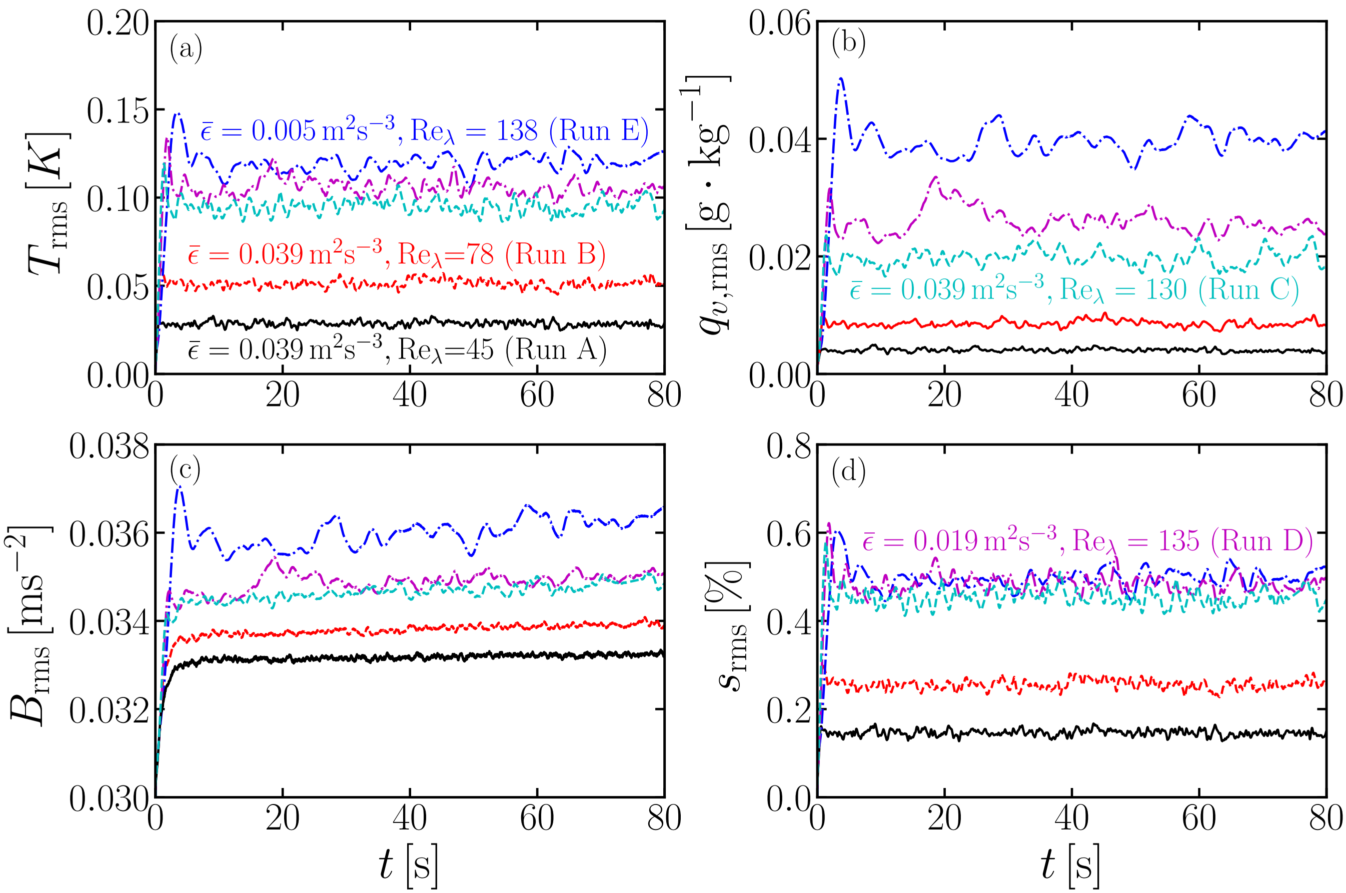

Figure 2. Time series of the field quantities: (a) T_{rms}, (b) q_v, rms, (c) B_{rms}, and (d) s_{rms}. Same simulations as in Figure 1.

written as

$$\frac{dA_i}{dt} = 2Gs. \tag{20}$$

It can be seen from Equation (20) that the evolution of the surface area is analogous to Brownian motion, indicating that its standard deviation $\sigma_A \propto \sqrt{t}$. A more detailed stochastic model for σ_A is developed by Sardina et al. (2015). Based on Equation (19), σ_A is given by

$$\frac{d\sigma_A^2}{dt} = \frac{d}{dt}\left\langle A'^2 \right\rangle = \frac{d}{dt}\left\langle A^2 - \langle A \rangle^2 \right\rangle = 4G\left\langle s' A' \right\rangle. \tag{21}$$

Sardina et al. (2015) adopted a Langevin equation to model the supersaturation field and the vertical velocity of droplets, resulting in the scaling law:

$$\sigma_A \sim C(\tau_L, \tau_{\mathrm{s}}, \mathrm{Re}_\lambda) t^{1/2}, \tag{22}$$

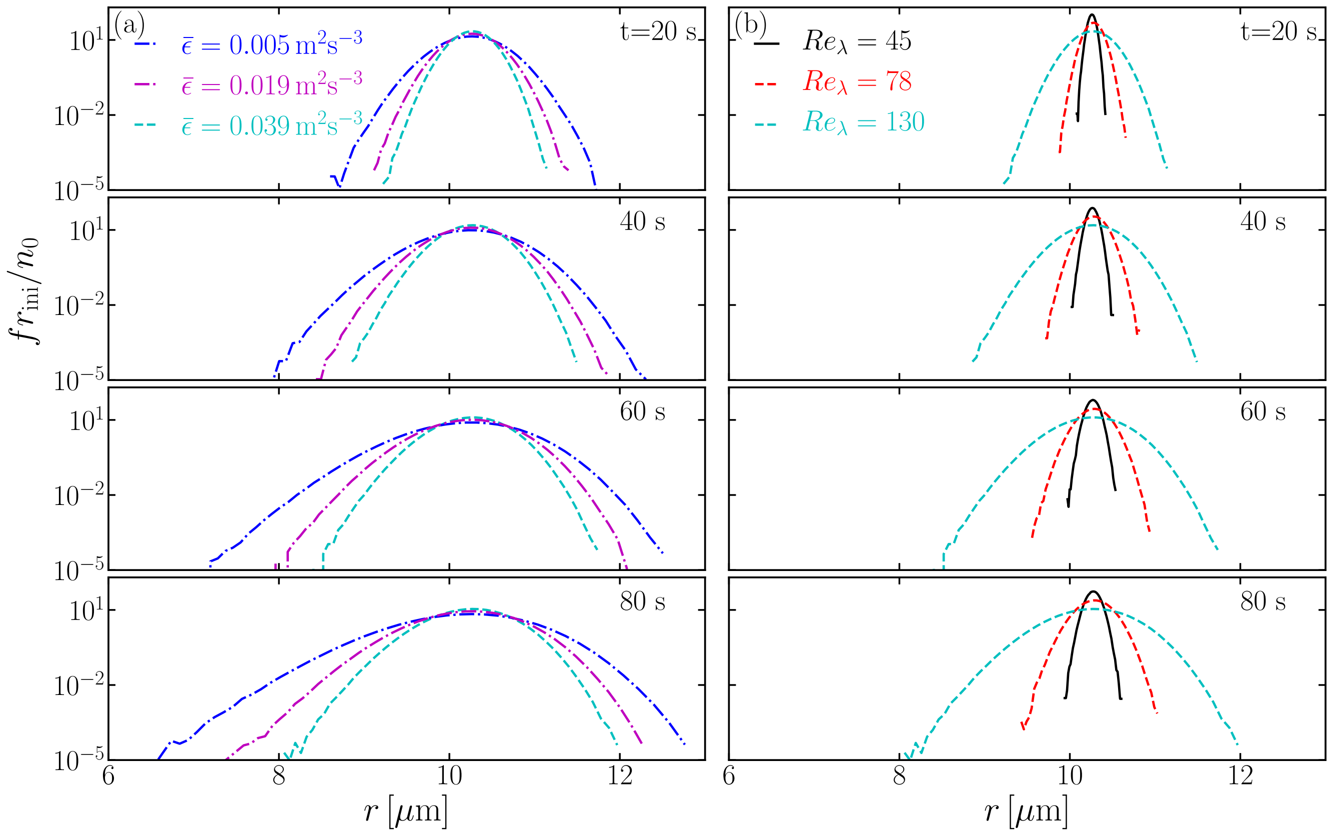

Figure 3. Comparison of the time evolution of droplet size distributions for different (a) $\bar{\epsilon}$ at $\mathrm{Re}_\lambda = 130$ (Runs C, D, and E in Table 2) and (b) Re_λ at $\bar{\epsilon} = 0.039\mathrm{m}^2\mathrm{s}^{-3}$ (Runs A, B, and C in Table 2). Same simulations as in Figure 1.

where $C(\tau_L, \tau_{\mathrm{s},\mathrm{Re}_\lambda})$ is a constant for given τ_L, τ_s, and Re_λ. Under the assumptions that $\tau_\mathrm{s} \ll T_L$ and a negligible influence on the macroscopic observables from small-scale turbulent motions, Sardina et al. (2015) obtained an analytical expression for σ_A as:

$$\sigma_A \sim \tau_\mathrm{s} \mathrm{Re}_\lambda t^{1/2}, \tag{23}$$

5 where τ_s is the phase transition time scale given by

$$\tau_\mathrm{s}^{-1}(t) = 4\pi G \int_0^\infty r f dr, \tag{24}$$

and τ_L is the turbulence integral time scale. The model proposed that condensational growth of cloud droplets depends only on Re_λ and is independent of $\bar{\epsilon}$. In terms of the size distribution $f(r,t)$, σ_A can be given as:

$$\sigma_A = \sqrt{a_4 - a_2^2}, \tag{25}$$

where a_ζ is the moment of the size distribution, which is defined as:

$$a_\zeta = \int\limits_0^\infty f\, r^\zeta \,\mathrm{d}r \Bigg/ \int\limits_0^\infty f \,\mathrm{d}r. \qquad (26)$$

Here, ζ is a positive integer. As shown in Figure 4, the time evolution of σ_A agrees with the prediction $\sigma_A \propto t^{1/2}$. Sardina et al. (2015) and Siewert et al. (2017) solved the passive scalar equation of s without considering fluctuations of T and q_v. Feedbacks to flow fields from cloud droplets were also neglected. They found good agreement between the DNS and the stochastic model. Comparing with Sardina et al. (2015) and Siewert et al. (2017), our study solve the complete sets of the thermodynamics of supersaturation. It is remarkable that a good agreement between the stochastic model and our DNS is observed. This indicates that the stochastic model is robust. On the other hand, modeling supersaturation fluctuations using the passive scalar equation seems to be sufficient for the Reynolds numbers considered in this study. We recall that τ_s in Equation (23) is constant. In the present study, τ_s is determined by Equation (24). Therefore, τ_s varies with time as shown in the inset of Figure 4(a). Nevertheless, since the variation of τ_s is small, we still observe $\sigma_A \sim t^{1/2}$ except for the initial phase of the evolution, where $s(t=0)=2\%$.

Comparing panels (a) and (b) of Figure 4, it is clear that changing Re_λ has a much larger effect on σ_A than changing $\bar{\epsilon}$. In fact, as $\bar{\epsilon}$ is increased by a factor of about 8, σ_A decreases only by a factor of about 1.6, so the ratio of their logarithms is about 1/5, i.e., $\sigma_A \propto \bar{\epsilon}^{-1/5}$. By contrast, σ_A changes by a factor of about 5 as Re_λ is increased by a factor of nearly 3, so $\sigma_A \propto \mathrm{Re}_\lambda^{3/2}$. This quantifies the high sensitivity of σ_A to changes of Re_λ compared to $\bar{\epsilon}$.

Two comments are here in order. First, we emphasize that we observe here $\sigma_A \propto \mathrm{Re}_\lambda^{3/2}$ instead of $\sigma_A \propto \mathrm{Re}_\lambda$. Therefore, there could be a critical Re_λ, beyond which $\sigma_A \propto \mathrm{Re}_\lambda$ and below which $\sigma_A \propto \mathrm{Re}_\lambda^{3/2}$. However, the highest Re_λ in our DNS is 130. To verify this proposal, a large parameter range of Re_λ is required. Second, we note that $\sigma_A \propto \bar{\epsilon}^{-1/5}$. This is because the Damköhler number increases with decreasing $\bar{\epsilon}$ (see Table 2), which is defined as the ratio of the fluid time scale to the characteristic thermodynamic time scale associated with the evaporation process $\mathrm{Da} = \tau_\mathrm{L}/\tau_\mathrm{s}$. Vaillancourt et al. (2002) also found that σ_A decreases with $\bar{\epsilon}$, even though the mean updraft cooling is included in their study.

5 Discussion and conclusion

Condensational growth of cloud droplets due to supersaturation fluctuations is investigated using DNS. Cloud droplets are tracked in a Lagrangian framework, where the momentum equation for inertial particles are solved. The thermodynamic equations governing the supersaturation field are solved simultaneously. Feedback from cloud droplets onto $\boldsymbol{u}$, T, and q_v is included through the condensation rate and buoyancy force. We resolve the smallest scale of turbulence in all simulations. Contrary to the classical condensation theory, which leads to a narrow distribution when supersaturation fluctuations are ignored, we find that droplet size distributions broaden due to supersaturation fluctuations. For the first time, we explicitly demonstrate that the size distribution becomes wider with increasing Re_λ, which is, however, insensitive to $\bar{\epsilon}$. Supersaturation fluctuations are subjected to both temperature fluctuations and water vapor mixing ratio fluctuations.

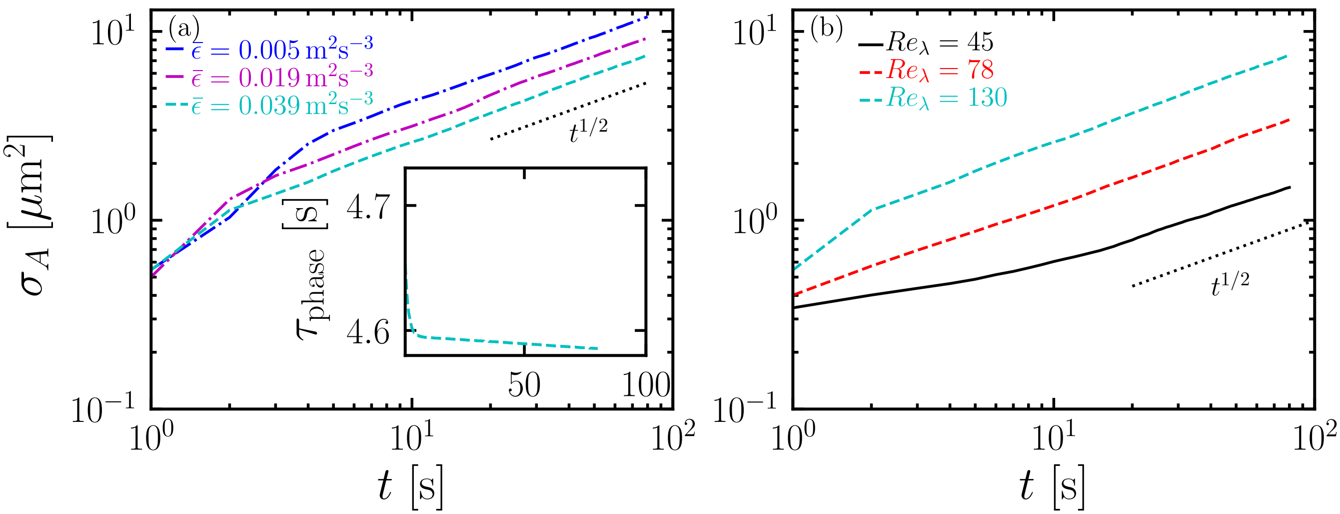

Figure 4. Time evolution of σ_A for different (a) $\bar{\epsilon}$ at $\mathrm{Re}_\lambda = 130$ and (b) Re_λ at $\bar{\epsilon} = 0.039\mathrm{m^2s^{-3}}$. Same simulations as in Figure 1.

We observe that $\sigma_A \propto \sqrt{t}$ when the complete sets of the thermodynamics equations governing the supersaturation are solved, which are consistent with the findings by Sardina et al. (2015) and Siewert et al. (2017). Even though fluctuations of temperature and water vapor mixing ratio, buoyancy force, and droplets feedbacks to the field quantities are neglected in their studies. This indicates that the stochastic model of condensational growth developed by Sardina et al. (2015) is robust. For the first time, to our knowledge, the stochastic model (Sardina et al., 2015) and simulation results from the complete set of thermodynamics equations governing the supersaturation field are compared. The broadening size distribution with increasing Re_λ demonstrates that condensational growth due to supersaturation fluctuations is an important mechanism for droplet growth. The maximum Re_λ in the present study is 130, which is about two orders of magnitude smaller than the one in atmospheric clouds ($\mathrm{Re}_\lambda = 10^4$). Since the width of the size distribution increases dramatically with increasing Re_λ, the supersaturation fluctuation facilitated condensation may easily overcome the bottleneck barrier (Grabowski and Wang, 2013).

The stochastic model developed by Sardina et al. (2015) assumes that the width of droplet size distributions is independent of $\bar{\epsilon}$. Our result shows that the width decreases slightly with increasing $\bar{\epsilon}$. However, the largest $\bar{\epsilon}$ in warm clouds is about $10^{-3}\,\mathrm{m^2s^{-3}}$ (Grabowski and Wang, 2013). Therefore, neglecting the smallest scales in the stochastic model is indeed acceptable. Vaillancourt et al. (2002) also found that the width of droplet size distribution decreases with increasing $\bar{\epsilon}$, which ranges from $1.9 \times 10^{-4}\,\mathrm{m^2s^{-3}}$ to $1.61 \times 10^{-2}\,\mathrm{m^2s^{-3}}$. However, their Re_λ varies at the same time as $\bar{\epsilon}$ changes from 12 to 34. It is unclear if their shrinking of the size distribution with increasing $\bar{\epsilon}$ is related to $\bar{\epsilon}$ or Re_λ. Nevertheless, their $\bar{\epsilon}$ changes by three orders of magnitude while their largest Re_λ is 34. Therefore, the contradiction between Vaillancourt et al. (2002) and the works of others (Paoli and Shariff, 2009; Lanotte et al., 2009; Sardina et al., 2015) could be related to poor scale separation in the simulations of Vaillancourt et al. (2002), who were unable to capture the effect of larger scales on condensational growth.

It could also be due to the mean updraft cooling included in the model of Vaillancourt et al. (2002), which was excluded in the present study and in the work of others. The present study may help resolve this contradiction.

In the present study, the simulation box is stationary, which means that the volume is not exposed to cooling, as no mean updraft is considered. Therefore, the condensational growth is solely driven by supersaturation fluctuations. This is similar to the condensational growth of cloud droplets in stratiform clouds, where the updraft velocity of the parcel is close to zero (Hudson and Svensson, 1995; Korolev, 1995). The observational data shows that the width of the size distribution is wider than the one expected from condensational growth with a mean supersaturation (Hudson and Svensson, 1995; Brenguier et al., 1998; Miles et al., 2000; Pawlowska et al., 2006; Siebert and Shaw, 2017a). Qualitatively consistent with observations, we show that the width of droplet size distributions broadens due to supersaturation fluctuations.

Entrainment of dry air is not considered here. It may lead to rapid changes of the supersaturation fluctuations and result in an even faster broadening of the size distribution (Kumar et al., 2014). Activation of aerosols in a turbulent environment is omitted. This may provide a more physical and realistic initial distribution of cloud droplets. Incorporating all the cloud microphysical processes is computationally demanding, and will have be explored in future studies.

Acknowledgements. We thank Wojtek Grabowski, Andrew Heymsfield, Gaetano Sardina, Igor Rogachevskii and Dhrubaditya Mitra for stimulating discussions. This work was supported through the FRINATEK grant 231444 under the Research Council of Norway, SeRC, the Swedish Research Council grants 2012-5797 and 2013-03992, the University of Colorado through its support of the George Ellery Hale visiting faculty appointment, and the grant "Bottlenecks for particle growth in turbulent aerosols" from the Knut and Alice Wallenberg Foundation, Dnr. KAW 2014.0048. The simulations were performed using resources provided by the Swedish National Infrastructure for Computing (SNIC) at the Royal Institute of Technology in Stockholm and Chalmers Centre for Computational Science and Engineering (C3SE). This work also benefited from computer resources made available through the Norwegian NOTUR program, under award NN9405K. The source code used for the simulations of this study, the PENCIL CODE, is freely available on https://github.com/pencil-code/.

References

Berry, E. X. and Reinhardt, R. L.: An analysis of cloud drop growth by collection: Part I. Double distributions, Journal of the Atmospheric Sciences, 31, 1814–1824, 1974.

Brenguier, J.-L., Bourrianne, T., Coelho, A. A., Isbert, J., Peytavi, R., Trevarin, D., and Weschler, P.: Improvements of droplet size distribution measurements with the Fast-FSSP (Forward Scattering Spectrometer Probe), Journal of Atmospheric and Oceanic Technology, 15, 1077–1090, 1998.

Chandrakar, K. K., Cantrell, W., Chang, K., Ciochetto, D., Niedermeier, D., Ovchinnikov, M., Shaw, R. A., and Yang, F.: Aerosol indirect effect from turbulence-induced broadening of cloud-droplet size distributions, Proceedings of the National Academy of Sciences, 113, 14 243–14 248, 2016.

Chen, S., Yau, M., and Bartello, P.: Turbulence effects of collision efficiency and broadening of droplet size distribution in cumulus clouds, J. Atmosph. Sci., 75, 203–217, 2018.

Devenish, B., Bartello, P., Brenguier, J.-L., Collins, L., Grabowski, W., IJzermans, R., Malinowski, S., Reeks, M., Vassilicos, J., Wang, L.-P., et al.: Droplet growth in warm turbulent clouds, Quart. J. Roy. Meteorol. Soc., 138, 1401–1429, 2012.

Götzfried, P., Kumar, B., Shaw, R. A., and Schumacher, J.: Droplet dynamics and fine-scale structure in a shearless turbulent mixing layer with phase changes, Journal of Fluid Mechanics, 814, 452–483, 2017.

Grabowski, W. W. and Abade, G. C.: Broadening of cloud droplet spectra through eddy hopping: Turbulent adiabatic parcel simulations, Journal of the Atmospheric Sciences, 74, 1485–1493, 2017.

Grabowski, W. W. and Wang, L.-P.: Growth of Cloud Droplets in a Turbulent Environment, Annu. Rev. Fluid Mech., 45, 293–324, 2013.

Haugen, N. E. L., Brandenburg, A., and Dobler, W.: Simulations of nonhelical hydromagnetic turbulence, Phys. Rev. E, 70, 016308, https://doi.org/10.1103/PhysRevE.70.016308, 2004.

Hudson, J. G. and Svensson, G.: Cloud microphysical relationships in California marine stratus, Journal of Applied Meteorology, 34, 2655–2666, 1995.

Johansen, A., Youdin, A. N., and Lithwick, Y.: Adding particle collisions to the formation of asteroids and Kuiper belt objects via streaming instabilities, Astron. Astroph., 537, A125, 2012.

Katzwinkel, J., Siebert, H., Heus, T., and Shaw, R. A.: Measurements of turbulent mixing and subsiding shells in trade wind cumuli, Journal of the Atmospheric Sciences, 71, 2810–2822, 2014.

Korolev, A. V.: The influence of supersaturation fluctuations on droplet size spectra formation, Journal of the atmospheric sciences, 52, 3620–3634, 1995.

Krüger, J., Haugen, N. E. L., and Løvås, T.: Correlation effects between turbulence and the conversion rate of pulverized char particles, Combustion and Flame, 185, 160–172, 2017.

Kumar, B., Schumacher, J., and Shaw, R. A.: Lagrangian Mixing Dynamics at the Cloudy–Clear Air Interface, Journal of the Atmospheric Sciences, 71, 2564–2580, https://doi.org/10.1175/JAS-D-13-0294.1, http://dx.doi.org/10.1175/JAS-D-13-0294.1, 2014.

Lamb, D. and Verlinde, J.: Physics and Chemistry of Clouds, Cambridge, England, Cambridge Univ. Press, 2011.

Lanotte, A. S., Seminara, A., and Toschi, F.: Cloud Droplet Growth by Condensation in Homogeneous Isotropic Turbulence, Journal of the Atmospheric Sciences, 66, 1685–1697, https://doi.org/10.1175/2008JAS2864.1, http://dx.doi.org/10.1175/2008JAS2864.1, 2009.

Li, X.-Y., Brandenburg, A., Haugen, N. E. L., and Svensson, G.: Eulerian and L agrangian approaches to multidimensional condensation and collection, J. Adv. Modeling Earth Systems, 9, 1116–1137, 2017.

Li, X.-Y., Brandenburg, A., Svensson, G., Haugen, N. E. L., Mehlig, B., and Rogachevskii, I.: Effect of Turbulence on Collisional Growth of Cloud Droplets, Journal of the Atmospheric Sciences, 75, 3469–3487, https://doi.org/10.1175/JAS-D-18-0081.1, https://doi.org/10.1175/JAS-D-18-0081.1, 2018.

Marchioli, C., Soldati, A., Kuerten, J., Arcen, B., Taniere, A., Goldensoph, G., Squires, K., Cargnelutti, M., and Portela, L.: Statistics of particle dispersion in direct numerical simulations of wall-bounded turbulence: Results of an international collaborative benchmark test, Intern. J. Multiphase Flow, 34, 879–893, 2008.

Miles, N. L., Verlinde, J., and Clothiaux, E. E.: Cloud droplet size distributions in low-level stratiform clouds, Journal of the atmospheric sciences, 57, 295–311, 2000.

Paoli, R. and Shariff, K.: Turbulent condensation of droplets: direct simulation and a stochastic model, Journal of the Atmospheric Sciences, 66, 723–740, 2009.

Pawlowska, H., Grabowski, W. W., and Brenguier, J.-L.: Observations of the width of cloud droplet spectra in stratocumulus, Geophysical research letters, 33, 2006.

Pope, S.: Turbulent Flows, Cambridge University Press, 2000.

Pruppacher, H. R. and Klett, J. D.: Microphysics of Clouds and Precipitation: Reprinted 1980, Springer Science & Business Media, 2012.

Saffman, P. G. and Turner, J. S.: On the collision of drops in turbulent clouds, J. Fluid Mech., 1, 16–30, https://doi.org/10.1017/S0022112056000020, http://journals.cambridge.org/article_S0022112056000020, 1956.

Saito, I. and Gotoh, T.: Turbulence and cloud droplets in cumulus clouds, New Journal of Physics, 2017.

Sardina, G., Picano, F., Brandt, L., and Caballero, R.: Continuous Growth of Droplet Size Variance due to Condensation in Turbulent Clouds, Phys. Rev. Lett., 115, 184501, https://doi.org/10.1103/PhysRevLett.115.184501, 2015.

Sardina, G., Poulain, S., Brandt, L., and Caballero, R.: Broadening of Cloud Droplet Size Spectra by Stochastic Condensation: Effects of Mean Updraft Velocity and CCN Activation, Journal of the Atmospheric Sciences, 75, 451–467, 2018.

Schiller, L. and Naumann, A.: Fundamental calculations in gravitational processing, Zeitschrift Des Vereines Deutscher Ingenieure, 77, 318–320, 1933.

Seinfeld, J. H. and Pandis, S. N.: Atmospheric chemistry and physics: from air pollution to climate change, John Wiley & Sons, 2016.

Shaw, R. A.: Particle-turbulence interactions in atmospheric clouds, Annu. Rev. Fluid Mech., 35, 183–227, 2003.

Shima, S., Kusano, K., Kawano, A., Sugiyama, T., and Kawahara, S.: The super-droplet method for the numerical simulation of clouds and precipitation: a particle-based and probabilistic microphysics model coupled with a non-hydrostatic model, Quart. J. Roy. Met. Soc., 135, 1307–1320, 2009.

Siebert, H. and Shaw, R. A.: Supersaturation fluctuations during the early stage of cumulus formation, Journal of the Atmospheric Sciences, 74, 975–988, 2017a.

Siebert, H. and Shaw, R. A.: Supersaturation fluctuations during the early stage of cumulus formation, Journal of the Atmospheric Sciences, 74, 975–988, 2017b.

Siewert, C., Bec, J., and Krstulovic, G.: Statistical steady state in turbulent droplet condensation, Journal of Fluid Mechanics, 810, 254–280, 2017.

Srivastava, R.: Growth of cloud drops by condensation: A criticism of currently accepted theory and a new approach, Journal of the atmospheric sciences, 46, 869–887, 1989.

Vaillancourt, P., Yau, M., and Grabowski, W. W.: Microscopic approach to cloud droplet growth by condensation. Part I: Model description and results without turbulence, Journal of the atmospheric sciences, 58, 1945–1964, 2001.

Vaillancourt, P., Yau, M., Bartello, P., and Grabowski, W. W.: Microscopic approach to cloud droplet growth by condensation. Part II: Turbulence, clustering, and condensational growth, Journal of the atmospheric sciences, 59, 3421–3435, 2002.

Veysey, II, J. and Goldenfeld, N.: Simple viscous flows: From boundary layers to the renormalization group, Rev. Modern Phys., 79, 883–927, 2007.

Yau, M. K. and Rogers, R.: A short course in cloud physics, Elsevier, 1996.